Calculation of the Solubility Limit of Ce in α-U and α-Zr by using First Principle Calculations and Phonon Calculations

Hyun Woo Seong[a], Ho Jin Ryu [a*],
[a] *Department of Nuclear & Quantum Engineering, Korea Advanced Institute of Science and Technology, 291 Daehakro, Yuseong, 34141, Republic of Korea*
[*] *Corresponding author: hojinryu@kaist.ac.kr*

1. Introduction

The metallic fuels are suitable for sodium-cooled fast reactor (SFR) than the oxide fuels. The metallic fuels contain low concentrations of Rare earth elements (REEs). REEs affect the metallic fuels. Main issue of REEs in the metallic fuels is the migration of REEs during irradiation. REEs tend to be redistributed to the outer region of fuel. The migration of REEs leads to the fuel-cladding chemical interaction (FCCI) [1,2]. The FCCI limits higher burnup of the fuel and causes fuel failure. Solid state diffusion is one of the candidates for the migration of REEs mechanism. In the solid-state diffusion mechanism, the solubility limit calculated from the phase diagram affects the driving force for diffusion within a dual phase field [3]. Therefore, the solubility limit of U-Zr-REEs and U-TRUs-Zr-REEs help understanding how REEs in the metallic fuels affect the distribution of constituent elements for performance analysis and safety assessment of metallic fuels. However, it is difficult to accurately measure the solubility limit in experiments. Furthermore, for radioactive materials, experiments are limited.

In recent decades, with the development of computers, computational simulations for material analysis have been developed in material science. The purpose of this study is to use computational simulation to complement the lack of experimental data. In this study, Ce is considered as a representative of REEs. At low temperature about 900K, stable phases of Ce, U, and Zr are of γ-Ce, α-U, and α-Zr, respectively. Therefore, in present work, we only focus on γ-Ce, α-U, and α-Zr phases. The solubility limits of γ-Ce in α-U and α-Zr are calculated by using first principles and phonon calculations.

2. Methods and Results

In the present work, the solubility limits of Ce in α-U and α-Zr are calculated by using first principles and phonon calculations. The details of these calculations are described in Section 2.1 and Section 2.2. The results of the solubility limits are shown in Section 2.3.

2.1 First principles

The first principles are based on DFT as implemented in the Vienna *ab initio* Simulation Package (VASP) [4,5]. The plane-wave basis set with an energy cutoff of 550eV within the framework of the projector augmented wave (PAW) method [6,7] is used to describe the valence electrons. The exchange-correlation functional parameterized in the generalized gradient approximation (GGA) [8] by Perdew, Burke, and Emzerhof (PBE) [9] is used. We treat $6s^26p^67s^25f^36d^1$ and $4s^24p^65s^24d^2$ as valence electrons for α-U and α-Zr, respectively. There is α-Ce that is more stable than γ-Ce at temperatures lower than 125K. Moreover, α-Ce and γ-Ce are same structure and DFT calculation is at 0K. Therefore, even if we simulate for γ-Ce, the result is for α-Ce. According to the Mott transition scenario [10], the $4f^1$ state of γ-Ce is considered more strongly localized than one of α-Ce. Therefore, we treat the [Xe] closed shell plus a single 4f state as core electrons and $5s^25p^66s^25d^1$ as valence electrons for γ-Ce. A Monkhorst-Pack k-points grid [11] is used for sampling of the Brillouin zone, with a 12×12×12 mesh, a 18×9×10 mesh, and a 16×16×10 mesh in γ-Ce, α-U, and α-Zr conventional cells, respectively. An equivalent density of k-points mesh is used for the supercells. The partial occupancies are set using the Methfessel-Paxton method [12] of order one with a smearing width of 0.2 eV. The electronic and ionic optimizations are performed using a Davidson-block algorithm [13] and a Conjugate-gradient algorithm [14], respectively. The stopping criteria for self-consistent loops are 0.1 meV/cell and 1 meV/cell tolerance of total energy for the electronic and ionic relaxation, respectively. All calculations are performed in the framework of non-spin-polarized and non-magnetic states. All calculations are relaxing all structural degrees of freedom (volume, ion position, and cell shape). The DFT calculation often fails to describe system with localized electrons. Therefore, the rotationally invariant DFT + U method [15] introduced by Dudarev et al. [16], Eq. (1)is used for $5f^3$ electrons in α-U with U_{eff} = 1.24 eV [17].

$$E_{DFT+U} = E_{DFT} + \frac{(U-J)}{2}\sum_{\sigma}\left[\left(\sum_{m_1}\hat{n}^{\sigma}_{m_1,m_2}\right) - \left(\sum_{m_1,m_2}\hat{n}^{\sigma}_{m_1,m_2}\hat{n}^{\sigma}_{m_2,m_1}\right)\right] \quad (1)$$

where on-site Coulomb interaction U, exchange parameter J, orbital moment m, spin σ, number of electrons occupying $\hat{n}^{\sigma}$, and effective value U_{eff} =U-J.

2.2 Phonon calculations

Force constants are computed using the density

functional perturbation theory (DFPT) [18] implemented in the VASP. The phonon calculations parameters are same as the first principles parameter (Section 2.1), except that the relaxing only the atomic position is performed in DFPT. These force constants are used to interpolate phonon dispersions to arbitrary wave vectors **q** by using the software Phonopy [19], which is based on the supercell method with finite displacements method [20]. Vibrational entropy is calculated with 101×101×101 **q** -points for all calculations by using Phonopy.

2.3 Solubility Limit

For binary system $A_{1-x}B_x$, the substitutional solubility limit of B-atoms in A-matrix, *s*, is calculated by seeking the minimum point of change in the Helmholtz free energy ($\Delta F^{\varphi}(x)$) as $\partial \Delta F^{\varphi}(s)/\partial s = 0$. Assuming the *s* is small, the *s* is obtained as in Eq. (2).

$$s = \exp\left(-\frac{\Delta E^{\varphi}_{mix}}{k_B T}\right)\exp\left(\frac{\Delta S^{\varphi}_{vib}}{k_B}\right) \quad (2)$$

where ΔE^{φ}_{mix} is mixing energy per solute atom as $x \to 0$ at φ phase, ΔS^{φ}_{vib} is change in vibrational entropy per solute atom as $x \to 0$ at φ phase, and k_B is Boltzmann constant.

For Ce-U and Ce-Zr system, substitutional alloy is dominant than interstitial alloy because the atomic size of Ce, U, and Zr are not significantly different. Also, the solubility limits of γ-Ce in α-U and α-Zr are small from phase diagrams [21,22]. Therefore, we can get the solubility limits of γ-Ce in α-U and α-Zr by using Eq. (2). In Eq. (2), ΔE^{φ}_{mix} can be calculated by first principles and ΔS^{φ}_{vib} can be calculated by phonon calculations.

To calculate mixing energy, orthorhombic $U_{N-1}Ce$ (N=16,32,48, and 64) and hcp $Zr_{N-1}Ce$ (N=16, 24, 36, and 54) supercells are used. The mixing energy per solute atom as $x \to 0$, ΔE^{φ}_{mix}, is obtained by linear regression. The results of the mixing energy per solute atom are represented in Fig. 1.

To calculate change in vibrational entropy, orthorhombic $U_{N-1}Ce$ (N=16 and 32) and hcp $Zr_{N-1}Ce$ (N=16 and 24) supercells are used because of computationally demanding using the DFPT method than first principle calculations. The entropy term is multiplied by the temperature to facilitate the analysis. Then we can interpolate it clearly with a linear function of temperature at temperatures above 300K and the change in vibrational entropy per solute atom is slope of this linear function of temperature. Finally, by using linear regression, the change in vibrational entropy per solute atom as $x \to 0$, ΔS^{φ}_{vib}, is obtained (Fig. 2). The information of linear regression functions of mixing energy and change in vibrational entropy about concentration of Ce are represented in Table I.

The solubility limits of γ-Ce in α-U and α-Zr is obtained by substituting mixing energy ΔE_{mix} and change in vibrational entropy ΔS_{vib} in Eq. (2). The solubility limits of γ-Ce in α-U is $\exp(-\frac{1.89}{k_B T} + 10.35)$ and the solubility limits of γ-Ce in α-Zr is $\exp(-\frac{0.70}{k_B T} + 2.66)$ that are shown in Fig. 3. For the U-Ce system, there is no data to compare with the calculated data. For the Zr-Ce system, the calculated solubility limits of γ-Ce in α-Zr is lower than experiments data [23] and previous phase diagram data [22].

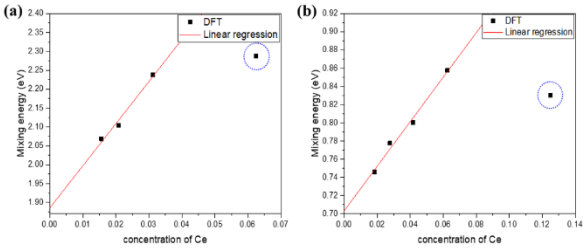

Fig. 1. The mixing energy and linear regression of (a) $U_{1-x}Ce_x$ and (b) $Zr_{1-x}Ce_x$.

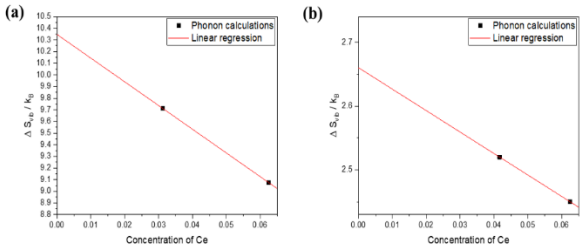

Fig. 2. Linear regression of the change in vibrational entropy of (a) $U_{1-x}Ce_x$ and (b) $Zr_{1-x}Ce_x$.

Table I: Parameter of linear regression functions

System	Function	Unit	Parameter
$U_{1-x}Ce_x$	$\Delta E_{mix}(x)$	eV	1.89 + 11.14x
	$\Delta S_{vib}(x)/k_B$	-	2.66 – 3.36x
$Zr_{1-x}Ce_x$.	$\Delta E_{mix}(x)$	eV	0.70 + 2.45x
	$\Delta S_{vib}(x)/k_B$	-	10.35 – 20.35x

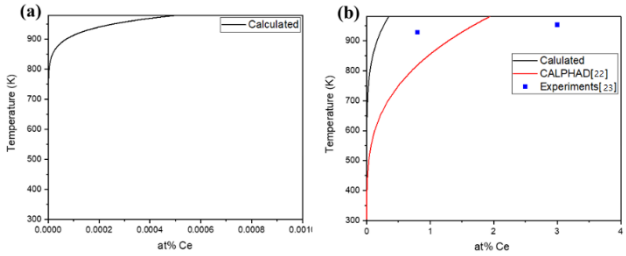

Fig. 3. Solubility limit of Ce in (a) U-Ce and (b) Zr-Ce

The reason why the calculated values differs from the experimental values is as follows. First, we assumed that

solubility limit is small and calculate solubility limits with the mixing energy and the change in vibrational entropy as $x \to 0$. In Table I, the values of the mixing energy and the change in vibrational entropy change according to the concentration of Ce, x. A very small x value does not affect to the values of the mixing energy and the change in vibrational entropy. The higher the value of x, the greater the influence on solubility limit. In Ce-Zr system, the solubility limit of Ce in Zr is not very small. Secondly, DFT is not accurate calculations on U and Ce. Therefore, we use another assumption to calculate U and Ce such as DFT+U method. For DFT+U method, previous literature [17] find U_{eff} =1.24eV by optimizing the results of α-U, β-U, and γ-U. However, only for α-U, the low U_{eff} is more accurate. In this study, U_{eff} =1eV is used to compare with U_{eff} =1.24eV (Table II). As shown in Fig. 4, the value of mixing energy changes as the U_{eff} value changes. Although the mixing energy difference is as small as 0.2eV, it has a large effect on solubility limit. Finally, vibrational entropy highly depends on the size of the supercell (Fig. 5). The lager supercell, the more similar to experimental data [24]. Since DFPT is very time consuming depending on supercell size, it is important to find the appropriate supercell size.

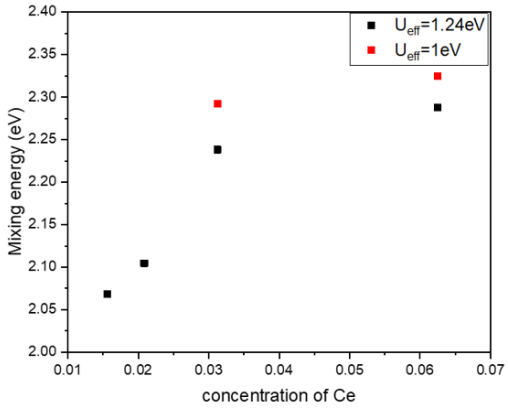

Fig. 4. Influence of U_{eff} in mixing energy of $U_{1-x}Ce_x$.

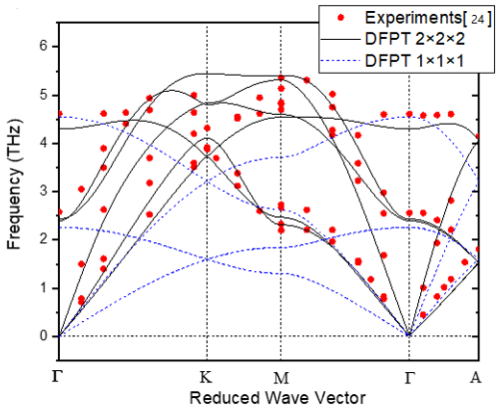

Fig. 5. Solubility limit of Ce in (a) U-Ce and (b) Zr-Ce

Table II: Volume and cohesive energy of α-U with U_{eff}

Phase		V/atom (Å^3)	E_C (eV/atom)
α-U	U_{eff} = 1.24eV	20.86	5.32
	U_{eff} = 1eV	20.71	5.64
	Exp.[a]	20.58	5.55

3. Conclusions

By using the first principles and the phonon calculations, the solubility limits of γ-Ce in α-U and α-Zr are obtained without experiments. The results of the first principles about pure γ-Ce in α-U and α-Zr are generally similar to experimental data. However, the results of the solubility limit of γ-Ce are different with experiments. There are several factors that affect solubility limit calculations; high solubility limit, U_{eff} value in DFT+U method, and supercell size.

REFERENCES

[1] Y.S. Kim, G.L. Hofman, A.M. Yacout, Migration of minor actinides and lanthanides in fast reactor metallic fuel, J. Nucl. Mater. 392 (2009) 164-170.
[2] R.G. Paul, C.E. Lahm, S.L. Hayes, Performance of HT9 clad metallic fuel at high temperature, J. Nucl. Mater. 204 (1993) 141-147.
[3] Y.S. Kim, S.L. Hayes, G.L. Hofman, A.M. Yacout, Modeling of constituent redistribution in U-Pu-Zr metallic fuel, J. Nucl. Mater. 359 (2006) 17-28.
[4] G. Kresse, J. Hafner, Ab initio molecular dynamics for liquid metals, Phys. Rev. B. 47 (1993) 558–561.
[5] G. Kresse, J. Furthmüller, Efficient iterative schemes for ab initio total-energy calculations using a plane-wave basis set, Phys. Rev. B - Condens. Matter Mater. Phys. 54 (1996) 11169–11186.
[6] P.E. Blöchl, Projector augmented-wave method, Phys. Rev. B. 50 (1994) 17953–17979.
[7] G. Kresse, D. Joubert, From ultrasoft pseudopotentials to the projector augmented-wave method, Phys. Rev. B - Condens. Matter Mater. Phys. 59 (1999) 1758–1775.
[8] D.C. Langreth, J.P. Perdew, Theory of nonuniform electronic systems. I.Analysis of the gradient approximation and a generalization that works, Phys. Rev. B. 21 (1980) 5469–5493.
[9] J.P. Perdew, K. Burke, M. Ernzerhof, Generalized gradient approximation made simple, Phys. Rev. Lett. 77 (1996) 3865–3868.
[10] B. Johansson, The α-γ transition in cerium is a mott transition, Philos. Mag. 30 (1974) 469–482.
[11] H.J. Monkhorst, J.D. Pack, Special points for Brillouin-zone integrations, Phys. Rev. B. 13 (1976) 5188-5192
[12] M. Methfessel, A.T. Paxton, High-precision sampling for Brillouin-zone integration in metals, Phys. Rev. B. 40 (1989) 3616–3621.

[13] K. Hirao, H. Nakatsuji, A generalization of the Davidson's method to large nonsymmetric eigenvalue problems, J. Comput. Phys. 45 (1982) 246–254.
[14] M.P. Teter, M.C. Payne, D.C. Allan, Solution of Schrodinger's equation for large systems, Phys. Rev. B. 40 (1989) 12255–12263.
[15] A.I. Liechtenstein, V.I. Anisimov, J. Zaanen, Density-functional theory and strong interactions: Orbital ordering in Mott-Hubbard insulators, Phys. Rev. B. 52 (1995) 5467–5471
[16] S. Dudarev, G. Botton, Electron-energy-loss spectra and the structural stability of nickel oxide: An LSDA+U study, Phys. Rev. B - Condens. Matter Mater. Phys. 57 (1998) 1505–1509.
[17] Correlation and relativistic effects in U metal and U-Zr alloy : Validation of ab initio approaches, 235128 (2013) 1–22
[18] Xavier Gonze and Changyol Lee, Dynamical matrices, Born effective charges, dielectric permittivity tensors, and interatomic force constants from density-functional perturbation theory, Phys. Rev. B 55, (1997) 10355-10368
[19] Atsushi Togo, Fumiyasu Oba, and Isao Tanaka, First-principles calculations of the ferroelastic transition between rutile-type and CaCl2-type SiO2 at high pressures, Phys. Rev. B, 78, (2008) 134106
[20] K. Parlinski, Z.Q. Li, Y. Kawazoe, First principles determination of the soft mode in cubic ZrO2, Phys. Rev. Lett. 78 (1997) 4063–4066.
[21] D.E. Janney, Metallic Fuels Handbook, Part 2: Elements and Alloys not Based on U-Zr, Pu-Zr, U-Pu, or U-Pu-Zr., (2018)
[22] N. Mattern, et. al., Experimental and thermodynamic assessment of the Ce-Zr system, Calphad Comput. Coupling Phase Diagrams Thermochem. 46 (2014) 213–219.
[23] I.R. HARRIS, G. V. Raynor, THE ELECTRONIC STATE OF CERIUM IN ZIRCONIUM-CERIUM ALLOYS, 6 (1964) 70–80.
[24] C. Stassis, J. Zarestky, D. Arch, O.D. McMasters, B.N. Harmon, Temperature dependence of the normal vibrational modes of hcp Zr, Phys. Rev. B. 18 (1978) 2632–2642.